This article was downloaded by: *[University of New Mexico]*
On: *10 May 2011*
Access details: *Access Details: [subscription number 792947466]*
Publisher *Taylor & Francis*
Informa Ltd Registered in England and Wales Registered Number: 1072954 Registered office: Mortimer House, 37-41 Mortimer Street, London W1T 3JH, UK

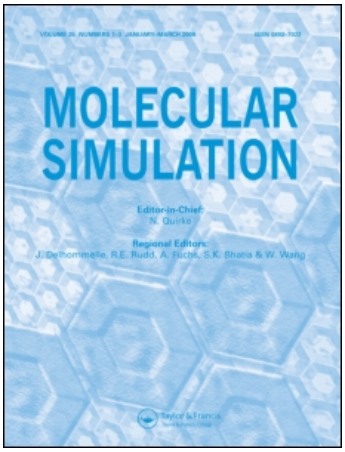

Molecular Simulation

Publication details, including instructions for authors and subscription information:
http://www.informaworld.com/smpp/title~content=t713644482

The chemically ordered glass: the limiting composition for chemical order in amorphous packings of hard-sphere mixtures

Peter Harrowell[a]; Julián R. Fernández[b]; D. B. Miracle[c]
[a] School of Chemistry, University of Sydney, New South Wales, Australia [b] Comisión Nacional de Energía Atómica, Buenos Aires, Argentina [c] Air Force Research Laboratory, Materials and Manufacturing Directorate, Dayton, OH, USA

Online publication date: 28 March 2011

To cite this Article Harrowell, Peter , Fernández, Julián R. and Miracle, D. B.(2011) 'The chemically ordered glass: the limiting composition for chemical order in amorphous packings of hard-sphere mixtures', Molecular Simulation, 37: 4, 293 — 298
To link to this Article: DOI: 10.1080/08927022.2010.548386
URL: http://dx.doi.org/10.1080/08927022.2010.548386

PLEASE SCROLL DOWN FOR ARTICLE

Full terms and conditions of use: http://www.informaworld.com/terms-and-conditions-of-access.pdf

This article may be used for research, teaching and private study purposes. Any substantial or systematic reproduction, re-distribution, re-selling, loan or sub-licensing, systematic supply or distribution in any form to anyone is expressly forbidden.

The publisher does not give any warranty express or implied or make any representation that the contents will be complete or accurate or up to date. The accuracy of any instructions, formulae and drug doses should be independently verified with primary sources. The publisher shall not be liable for any loss, actions, claims, proceedings, demand or costs or damages whatsoever or howsoever caused arising directly or indirectly in connection with or arising out of the use of this material.

Molecular Simulation
Vol. 37, No. 4, April 2011, 293–298

Taylor & Francis
Taylor & Francis Group

The chemically ordered glass: the limiting composition for chemical order in amorphous packings of hard-sphere mixtures

Peter Harrowell[a]*, Julián R. Fernández[b] and D.B. Miracle[c]

[a]*School of Chemistry, University of Sydney, New South Wales 2006, Australia;* [b]*Comisión Nacional de Energía Atómica, Av. Libertador 8250, Capital Federal, Buenos Aires, Argentina;* [c]*Air Force Research Laboratory, Materials and Manufacturing Directorate, Wright-Patterson AFB, 2230 Tenth St, Dayton, OH 45433, USA*

(*Received 18 September 2010; final version received 13 December 2010*)

We consider the limits of chemical order (i.e. avoidance of solute–solute contact) in amorphous close-packed mixtures of hard spheres of two different sizes. The upper bound on the solute concentration, beyond which solute–solute contact cannot be avoided, is determined for a range of particle size ratios. Scaling the composition by this limiting value is found to collapse plots of the solute coordination and mixture energies as a function of composition for different values of size ratios onto a single master curve. A number of features of the behaviour of amorphous alloys in the vicinity of this limiting concentration are discussed.

Keywords: glass transition; random close packing; amorphous alloys

Downloaded By: [University of New Mexico] At: 19:04 10 May 2011

1. Introduction

In this paper, we shall consider the consequences of chemical order imposed on a dense amorphous mixture of hard spheres of two different sizes. Chemical order refers here to the tendency of the solute (here defined as the minority species) to avoid contact with other solute particles. Chemical ordering of this kind characterises some important classes of glass-forming liquids. The network glass former, silica, represents a near-perfect example of chemical order in which the silicon atoms scrupulously avoid bonding directly with other silicon atoms. The first well-studied examples of amorphous alloys comprise metal and metalloid components in which the metalloid–metalloid contacts are avoided [1]. Although the hard-sphere model we shall employ in this study is inadequate for quantitative modelling of these specific systems, it is useful for clarifying the fundamental consequences of coupling compositional fluctuations to the structural variations in the problem of dense packing. The efficient cluster packing (ECP) model was developed [2–4] from such a perspective. In the ECP model, one considers the packing, not of the individual spherical particles, but of the (overlapping) solute coordination clusters. The solute coordination clusters are regarded as identifiable elementary structural units due, explicitly, to the solute–solute avoidance imposed by the chemical ordering condition.

Previously, we have examined the ECP model from the point of view of its packing efficiency [5]. In this paper, we address the more general aspects of the constraints that chemical order imposes on the structure of amorphous packings of binary mixtures of spheres. Our results are as follows. We begin by identifying, in amorphous packings, a limiting value of the solute composition (expressed as the solute mole fraction $x_B = N_B/(N_A + N_B)$) above which solute–solute contacts are unavoidable. We determine the dependence of this limiting composition, x_B^*, on the ratio $R = r_B/r_A$ of sphere radii. We demonstrate that x_B^* provides a general scaling for the composition dependence of nearest-neighbour contacts and properties such as potential energy that depends on these local correlations. We establish the topological constraints of the coordination shell overlap arising from chemical order and, finally, we consider the implications of these results with regard to glass-forming ability of chemically ordered alloys.

2. Method

To construct high-density amorphous packings of binary hard-sphere mixtures, we have used the algorithm described by Clarke and Wiley [6] with some modifications relating to the imposition of chemical order. The packing fraction η of a system of hard spheres with no overlap and m components is defined as follows:

$$\eta = \frac{4\pi}{3}\frac{\sum_{i=1}^{m} N_i r_i^3}{V}, \tag{1}$$

where N_i and r_i are the number and radius of component i, and V is the volume of the simulation cell. Periodic boundary

*Corresponding author. Email: peter@chem.usyd.edu.au

ISSN 0892-7022 print/ISSN 1029-0435 online
© 2011 Taylor & Francis
DOI: 10.1080/08927022.2010.548386
http://www.informaworld.com

Downloaded By: [University of New Mexico] At: 19:04 10 May 2011

conditions are applied. The overlap S between a pair of neighbouring particles is defined as the sum of their radii minus the distance between the centres (Figure 1). For a given configuration, the overlap can be reduced by moving the i sphere along a vector $\mathbf{t}_i$, the sum of the individual pairwise overlap vectors whose individual magnitudes are equal to the appropriate value of S, as shown in Figure 1. We can identify, for a specific configuration, the maximum value of the pairwise overlaps as $S_{\max}$. Particles are moved one at a time in a sequence determined by the random construction of the initial configuration. Each move is accepted if no value of S in the new configuration exceeds $S_{\max}$ of the old configuration. For each accepted configuration, $S_{\max}$ is re-determined. If $S > S_{\max}$, $\mathbf{t}_i$ is reduced by half every attempt until the movement is accepted. This process continues until the maximum overlap $S_{\max}$ is less than $10^{-5} r_A$. At this point, the simulation box lengths are reduced by a factor $f_1 < 1$ to generate new overlaps; then, the whole previous process is repeated. If, after several attempts, $S_{\max}$ cannot be reduced by moving the spheres according to $\mathbf{t}_i$ or at random, the box lengths are increased by a factor $f_2 > 1$, such that $f_1 f_2 < 1$.

We impose chemical order through the construction of the initial configuration and through the use of a two-step process for maximising density. In the spirit of the ECP model [2], we begin our construction of the initial configuration by first generating a random closed-packed configuration of the solute particles, labelled B, on their own. This initial configuration is then isotopically expanded to allow for space to add the majority solvent species, labelled A. This procedure is designed to provide the highest density disordered arrangement of solutes in which all solute–solute contact is explicitly forbidden. The empty space between B spheres is filled up with A spheres allowing an overlap S not larger than a maximum value $S_{\max}$. The random generation of A spheres is repeated a large number of times ($\sim 10^6$). The total number of A spheres, N_A, can be controlled through the volume of the simulation cell.

If all spheres are allowed to move directly from this initial configuration, some solute–solute contacts will occur as a consequence of the relaxation. To further minimise the number of these contacts, we adopted a two-stage relaxation process. In the first stage, only the A solvent spheres are moved, using the Clarke–Wiley algorithm, in a sequential fashion, whereas the solute spheres are kept at their initial positions. This will accommodate the A spheres around the solutes so as to eliminate or reduce the gaps between spheres as much as possible. In the second stage, and once the system has achieved a certain value of η or after several relaxation steps, all spheres are moved regardless of their type.

We have also generated random alloys in which A and B particles are added randomly to the simulation cell, and both species are moved to maximise density without any species–specific constraints being applied.

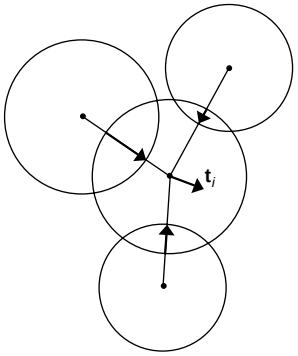

Figure 1. Sketch of the movement of sphere i along the vector sum of overlaps $\mathbf{t}_i$.

3. Results: the critical solute concentration x_B^*

The 'loss' of chemical order can be measured by the increase in the average number of solute–solute contacts per solute, a number that is zero in the absence of BB contacts (i.e. perfect chemical order) and increases as contacts appear. Let Z_{BB} be the mean number of BB contacts per B particle and Z_{BA} be the mean number of A neighbours per B particle. Similarly, Z_{AA} and Z_{AB} correspond to the mean number of A and B neighbours, respectively, per A particle. In Figure 2, we plot Z_{BB} as a function of x_B for a range of radius ratios using the protocol described in the previous section. The constraint that BB contacts are avoided is manifest in the persistence of $Z_{BB} \sim 0$ for small x_B. (A random arrangement without this constraint would see Z_{BB} increase linearly for small x_B.) There clearly is a limit to how large x_B can be before BB contacts become unavoidable. To understand the

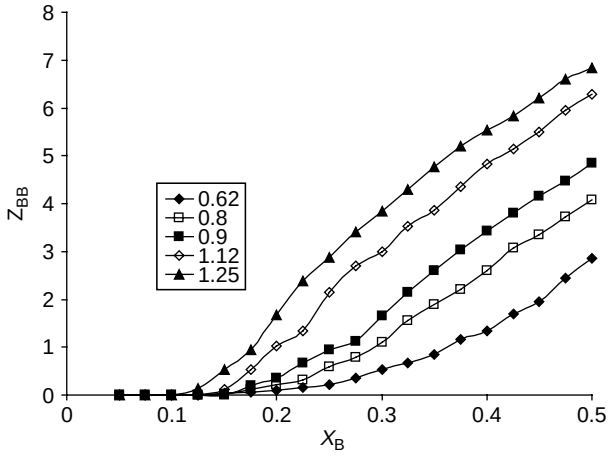

Figure 2. The average number Z_{BB} of B neighbours per B particle as a function of the solute mole fraction x_B for five different radius ratios, $R(= r_B/r_A) = 0.62$, 0.8, 0.9, 1.12 and 1.25.

Downloaded By: [University of New Mexico] At: 19:04 10 May 2011

geometrical nature of this compositional limit, we consider the following. Starting with the identity,

$$N_B Z_{BA} = N_A Z_{AB}, \tag{2}$$

we note that, in the absence of any BB contacts, Z_{BA} is a constant (let us call it z_B^o), equal to the coordination number of a B particle with only A neighbours. We can then rewrite Equation (2) as

$$\frac{x_B}{1 - x_B} = \frac{Z_{AB}}{z_B^o}. \tag{3}$$

The maximum value of x_B is, from Equation (3), determined by the critical value of Z_{AB}, i.e. how many B's can you fit into the coordination polyhedron around an A particle before BB contacts become unavoidable. This upper bound on a chemically ordered Z_{AB} is typically well below half of the particles coordinating the solute. An icosahedron (12 vertices), for example can only accommodate three separated B particles so the critical value of Z_{AB} for an icosahedral coordination shell is 3.

We shall define the critical solute fraction x_B^* as the composition at which Z_{AB} reaches its critical value, i.e. Z_{AB}^*. Now all that remains is to determine Z_{AB}^*. How many non-contacting B particles one can accommodate around an A particle is a well-posed geometrical problem that deserves attention. We shall not attempt a detailed treatment of this problem but, rather, employ the following simple heuristic based on the average *total* coordination number z_A about an A particle. As we make the radius ratio $R = r_B/r_A$ smaller or larger than 0.9022, z_A increases or decreases from the value of 12. The calculated values of z_A as a function of x_B, illustrating this point, have been plotted in Figure 3 for five values of R. Our strategy for determining Z_{BA}^* is to assign a representative topology for each integer value of z_A, neglecting the topological consequences of particles of different size in the coordination shell. Our question, then, is what cluster topologies do we choose?

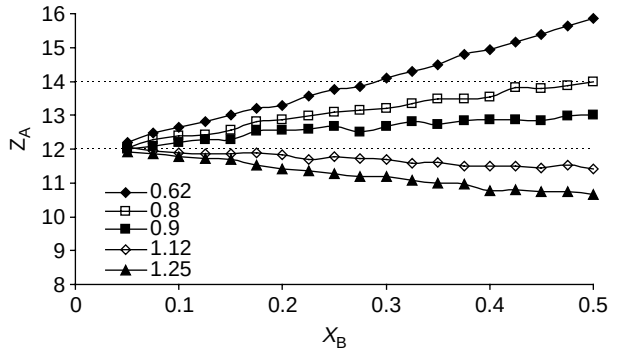

Figure 3. The average total coordination number z_A per A particle plotted against x_B for five different radius ratios, $R(= r_B/r_A) = 0.62$, 0.8, 0.9, 1.12 and 1.25.

There is a considerable body of literature arguing that liquids of spherical particles are dominated by polytetrahedral arrangements [7–10]. In terms of coordination polyhedra, this means focusing on polyhedra with all faces triangular. In Table 1, we present a list of triangulated polyhedra with coordination numbers ranging from 10 to 16, the range we observe in our packing calculations (Figure 3). For each cluster topology, we have determined Z_{AB}^* as the maximum number of sites that can be coloured so that no two coloured sites are neighbours.

Table 1 provides the basis for a relationship between the coordination number and the critical solute number Z_{AB}^*. In the analysis that follows, we have used a linear interpolation for the value of Z_{AB}^* when the average coordination number lies between 12 and 14.

This estimate of Z_{AB}^*, while capturing the essential aspect that the quantity increases from three with increasing coordination number, clearly neglects a number of details. One feature is worth pointing out for future study. One 'strategy' for increasing Z_{AB}^* is to introduce quadrilateral faces in the coordination polyhedra because the associated reduction of bonds makes the 'no-solute-neighbours' constraint easier to meet. For example, the densest packed cluster with 14 (equivalent) spheres in the coordination shell is not the triangulated Frank–Kasper cluster cited above but one with eight triangular faces and eight quadrilateral ones [11]. For this cluster, $Z_{AB}^* = 6$. The significance of being the densest packed cluster aside, this observation suggests that any influence that favours maximising the number of AB interactions may have the effect of destabilising polytetrahedral structures in favour of those with a significant number of fourfold rings.

In Figure 3, we plot the calculated value of the average total coordination number z_A about the A particles vs. x_B for sphere mixtures with different radius ratios R. Horizontal lines at $z_A = 12$ and 14 mark the concentrations over which the A coordination transitions from being able to accommodate a maximum of three B particles to four B particles (as estimated by the scheme described above). We now have an implicit expression for the critical value of Z_{AB} as a function of x_B for a number of choices of R. For $R = 1.12$ and 1.25, z_A never exceeds 12 and so $Z_{AB}^* = 3$ for all values of x_B. For $R = 0.9$ and 0.8, z_A lies between 12 and 14 over the studied composition range and so, invoking the

Table 1. The maximum number Z_{AB}^* of isolated B particles accommodated by triangulated coordination polyhedra over a range of coordination numbers.

Coordination number	Polyhedron	Z_{AB}^*
10	Bicapped square antiprism	3
12	Icosahedron	3
14	Frank–Kasper cluster [14]	4
15	Frank–Kasper cluster [14]	4
16	Frank–Kasper cluster [14]	4

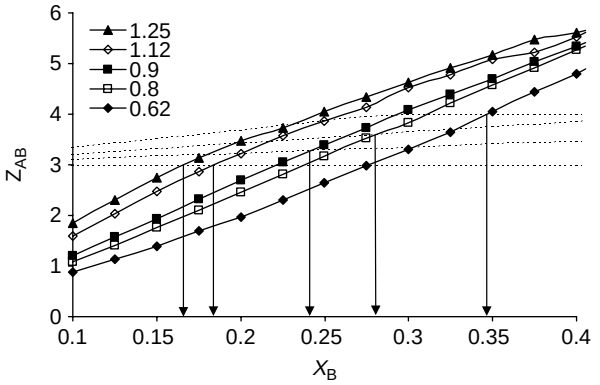

Figure 4. The calculated Z_{AB} (solid curve and points) is plotted against x_B along with the value of limiting value Z^*_{AB} (dashed curves) using the interpolation (described in text) of the data in Table 1. The intersection of the two curves – Z_{AB} and Z^*_{AB} – for each value of R determines the value of the limiting composition x^*_B, indicated by an arrow for each value of R.

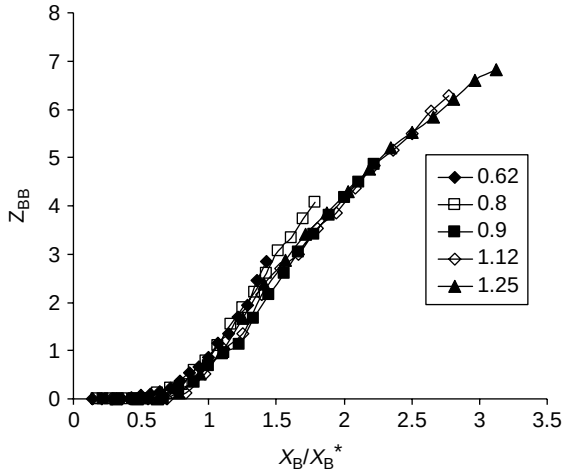

Figure 5. The average number Z_{BB} of B neighbours per B particle as a function of the reduced solute mole fraction x_B/x^*_B for five different radius ratios, $R(= r_B/r_A) = 0.62$, 0.8, 0.9, 1.12 and 1.25.

linear interpolation of Z^*_{AB} from 3 to 4 over this range of z_A, we have $Z^*_{AB} = 3 + 1.2x_B$ (for $R = 0.9$) and $Z^*_{AB} = 3 + 2.18x_B$ (for $R = 0.8$). Finally, for $R = 0.62$, $z_A = 14$ at $x_B \approx 0.285$. For x_B greater than this value, $Z^*_{AB} = 4$, whereas below this composition, we have $Z^*_{AB} = 3 + 3.51x_B$. In Figure 4, we have plotted each of these estimates of the limiting value Z^*_{AB} alongside the calculated value of Z_{AB}. The point at which, for each value of R, the two lines, Z^*_{AB} and Z_{AB}, intersect corresponds to the value of the critical composition x^*_B, the composition above which solute–solute becomes unavoidable. In Table 2, we list the values of R and x^*_B along with the values of z_A at the critical composition and Z^*_{AB}.

In Figure 5, we plot the different Z_{BB} curves against the composition reduced by the critical value x^*_B. The curves are found to collapse onto a single master curve. This remarkable result implies that it is possible to capture the role of the size difference in determining the number of solute–solute contacts simply through the introduction of a reference concentration. The dependence of the critical concentration x^*_B on the radius ratio R reflects the fact that, as the solute size increases, the mixture can accommodate fewer solutes before the solvating A particles have been exhausted and solute–solute contact becomes unavoidable. Before leaving Figure 5, we note that BB contacts appear (i.e. Z_{BB} begins to increase from 0) at compositions less than x^*_B. The critical composition establishes the composition at which BB contacts are unavoidable but it does not establish the composition at which the contacts begin to appear because the latter quantity depends on the details of how the chemical order is stabilised or selected for. The argument presented here simply precludes the possibility of $Z_{BB} = 0$ for $x_B > x^*_B$.

Table 2. The values presented are of the critical solute concentration x^*_B above which solute–solute contact becomes unavoidable in the binary hard-sphere glass for a number of different values of the radius ratio $r_B/r_A = R$. Also presented are the values of z_A and Z^*_{AB} at x^*_B.

R	x^*_B	z_A	Z^*_{AB}
0.62	0.345	14.5	4
0.8	0.28	13.15	3.6
0.9	0.24	12.6	3.3
1.12	0.18	11.85	3
1.25	0.16	11.6	3

Does the critical composition x^*_B provide a useful scaling of quantities associated with quantities other than Z_{BB}? A simple model of the energetics of a binary mixture can be expressed in an energy function of the form:

$$\frac{E}{N} = -\frac{e_{AA}}{2}(1 - x_B)Z_{AA} - e_{AB}x_BZ_{BA} - \frac{e_{BB}}{2}x_BZ_{BB}. \quad (5)$$

To pick parameters consistent with chemical ordering, we select $e_{AA} = 1.0$, $e_{AB} = 1.5$ and $e_{BB} = 0$. In Figure 6, we plot E/N for a range of compositions and size ratios, using the values of Z_{AA} and Z_{BA} obtained from the hard-sphere simulations. We note the presence of a minimum value in each curve. Although the position and depth of this minimum depends on the specific choice of the interaction strengths e_{AA}, e_{AB} and e_{BB}, the existence of the minimum value is a generic consequence of interactions that favour chemical order. The energy decreases as x_B increases from zero due to the increasing number of AB contacts. Once the composition has increased to the point that BB contacts are being formed, the energy begins to increase again due to the associated decrease in the number of both AA and AB contacts. In Figure 7, we replot E/N against the

Downloaded By: [University of New Mexico] At: 19:04 10 May 2011

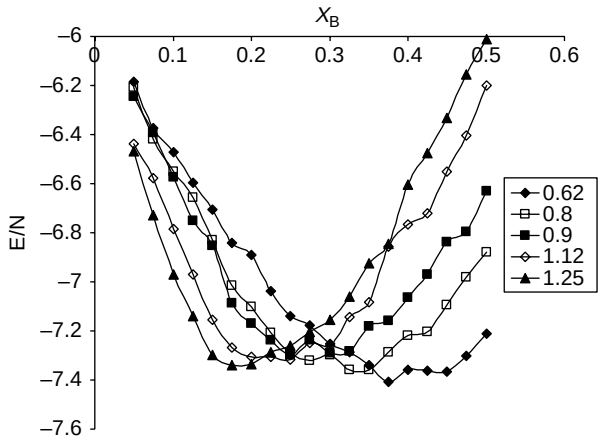

Figure 6. The average potential energy per particle *E*/*N* as a function of x_B for the five values of *R*. *E*/*N* was calculated using Equation (5) and the following values: $e_{AA} = 1.0$, $e_{AB} = 1.5$ and $e_{BB} = 0.0$.

reduced mole fraction x_B/x_B^*. Again, we obtain a remarkable collapse of the data onto a single master curve with a minimum at $x_B/x_B^* \sim 1.1$. It is reasonable, based on the type of analysis presented here, to propose that the critical concentration is likely to lie close to the eutectic point.

4. On the consequences of chemical order

In a chemically ordered alloy, the solute particles (B) have only solvent (A) in their coordination shell. An overlap of two solute coordination shells, therefore, corresponds to one or more A particles that have both solutes as neighbours. At the limiting concentration, x_B^* the number of B neighbours per A particle, Z_{AB} (listed in Table 1) are

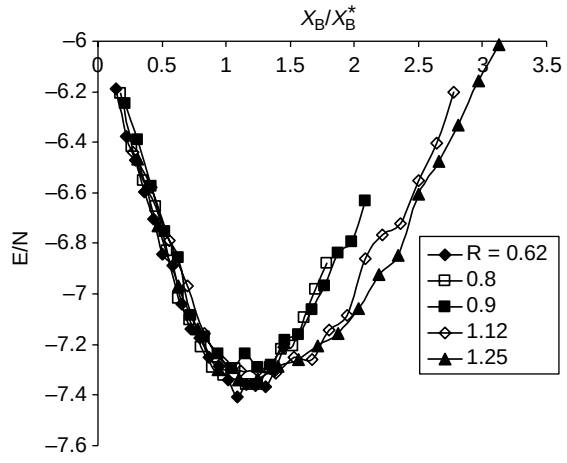

Figure 7. The average potential energy per particle *E*/*N* plotted as a function of the reduced composition x_B/x_B^* for the five values of *R*. The details of the calculation of *E*/*N* are the same as in Figure 6.

maximal which means that considerable constraints are imposed on the geometrical arrangement of these particles' solutes so as to avoid one another. A brief play with polyhedra models is enough to convince one that solutes are organised either in a roughly trigonal planar ($Z_{AB}^* = 3$) or in a tetrahedral or square planar ($Z_{AB}^* = 4$) arrangement about the A particle so as to avoid solute–solute contact. Chemical order, in other words, generates geometric order when pushed towards the limiting composition. Let us consider the crystal structure at the limiting concentration for $R = 1$ in the fcc crystal, the $AuCu_3$ structure. The structure consists of staggered hexagonal packed planes of A_3B composition as sketched in Figure 8. When the layers above and below are included, each white (A) particle is coordinated by four Bs, arranged about the A as a planar. That $Z_{AB}^* = 4$ rather than the 3 we used for random packings with $R > 0.8$ is because the coordination polyhedra of the fcc crystal is a cube octahedron which has square faces as well as triangular ones, whereas in the disordered packing, we assumed that the coordination polyhedra were fully triangulated.

Crystallisation increases, often substantially, the critical composition over its value in the amorphous state. This increase is largely due to the topology of crystal lattices which often include four- and/or six-sided rings, instead of the three-sided rings of the triangulated coordination shells we have used to model the amorphous topology. At a radius ratio of 1, for example, the stable crystal will be a chemically ordered fcc structure. Such substituted fcc structures can be formed up to a composition of $x_B = 0.25$, corresponding to the $AuCu_3$ structure, before solute–solute contact becomes inevitable. This is an increase over the value of $x_B^* \sim 0.20$ for the amorphous packing at $r_B/r_A = 1$. At $r_B/r_A \sim 0.6$, the value below which crystal packing fractions in excess of the fcc value is the norm, there are chemically ordered crystals with compositions A_3B (i.e. Fe_3C), A_2B (i.e. CdI_2) and even up to AB (i.e. CrB). It is not obvious why many of the optimally packed crystals of two different spheres satisfy the constraint of chemical order. In contrast, we find $x_B^* = 0.35$ for $R = 0.62$ in the amorphous packing of the two hard spheres.

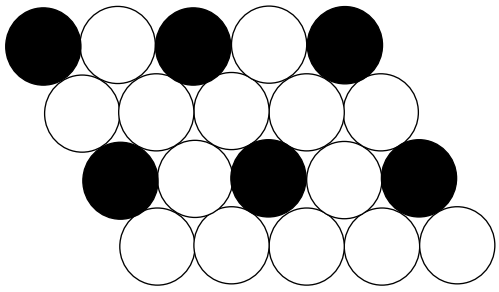

Figure 8. The maximal packing of solute particles without solute–solute contact in a 2D triangular crystal.

Downloaded By: [University of New Mexico] At: 19:04 10 May 2011

Downloaded By: [University of New Mexico] At: 19:04 10 May 2011

Inoue et al. [12,13] have identified negative heats of mixing among the elemental constituents (along with significant differences in radii) as a key characteristic of bulk glass-forming alloys. This condition is also just what is required to stabilise chemical order as we have described it here. It is tempting to associate the critical composition with good glass-forming ability on the grounds that we would expect this composition to be associated with a minimum in the enthalpy of the amorphous state. This suggestion, however, falls short of explaining why the maximum crystallisation rate should be decreased at the critical composition. If composition fluctuations in the amorphous state were minimised around the critical composition x_B^*, then we might have the basis of an explanation of high glass-forming ability. Crystallisation from a mixture will always involve composition fluctuations – except when either (i) the mixture composition just happens to coincide with that of the crystal (a special case) or (ii) the particle size differences are small enough to allow random substitution in the crystal (a situation we explicitly exclude in glass-forming alloys). The indications from this study that the critical composition lies near the minimum potential energy with respect to composition are consistent with the proposal that composition fluctuations might exhibit a minima around x_B^*. This proposal, that glass-forming ability in alloys depends on the amplitude of compositional fluctuations in the liquid and that the critical composition, identified for the first time in this paper, corresponds to a minimum in these fluctuations, is the one that is worth further study.

5. Conclusions

Chemical order, referring here to the avoidance of contacts between members of at least one chemical species in an atomic mixture, provides a generic form of organisation, even in amorphous materials. In this paper, we have argued that the limiting composition x_B^*, the composition above which chemical order must be violated, represents an important characteristic of amorphous mixtures. We have demonstrated that the composition-dependent, species-dependent coordination numbers for different radius ratios collapse onto a single master curve when the composition is scaled by the limiting composition. Other properties such as potential energy that depend on these coordination numbers show a similar scaling behaviour with regard to x_B^*. These observations lead us to a rather surprising conclusion that most of the important geometrical consequences of packing spheres of different sizes can be captured by a single quantity, the limiting composition.

Acknowledgements

P. H. gratefully acknowledges valuable discussions with Toby Hudson. This work has been supported by funding from the Discovery Program of the Australian Research Council.

References

[1] F. Spaepen and D. Turnbull, *Metallic glasses*, Ann. Rev. Phys. Chem. 35 (1984), pp. 241–263.
[2] D.B. Miracle, *A structural model for metallic glasses*, Nat. Mater. 3 (2004), pp. 697–702.
[3] D.B. Miracle, *The efficient cluster packing model – An atomic structural model for metallic glasses*, Acta Mater. 54 (2006), pp. 4317–4336.
[4] D.B. Miracle, D. Louzguine-Luzgin, L. Louzguina-Luzgina, and A. Inoue, *An assessment of binary metallic glasses: Correlations between structure, glass forming ability and stability*, Int. Mater. Rev. 55 (2010), pp. 218–258.
[5] A.N. Alcaraz, R.S. Duhau, J.R. Fernández, P. Harrowell, and D.B. Miracle, *Dense amorphous packing of binary hard sphere mixtures with chemical order: The stability of a solute ordered approximant*, J. Non-Cryst. Solids 354 (2008), pp. 3171–3178.
[6] A.S. Clarke and J.D. Wiley, *Numerical simulation of the dense random packing of a binary mixture of hard spheres: Amorphous metals*, Phys. Rev. B 35 (1987), pp. 7350–7357.
[7] D.R. Nelson, *Polytetarhedral order in condensed matter*, Solid State Phys. 42 (1989), pp. 1–90.
[8] J.-F. Sadoc and R. Mosseri, *Geometric Frustration*, Cambridge University Press, Cambridge, MA, 1999.
[9] J.P.K. Doye, *A model metal potential exhibiting polytetrahedral clusters*, J. Chem. Phys. 119 (2003), pp. 1136–1148.
[10] A.V. Anikeenko and N.N. Medvedev, *Polytetrahedral nature of the dense disordered packings of hard spheres*, Phys. Rev. Lett. 98 (2007), 235504(1–4).
[11] D.B. Miracle, E.A. Lord, and S. Ranganathan, *Candidate atomic cluster configurations in metallic glass structures*, Mater. Trans. 47 (2006), pp. 1737–1742.
[12] A. Inoue, T. Zhang, and T. Masumoto, *Glass-forming ability of alloys*, J. Non-Cryst. Solids 156–158 (1993), pp. 473–480.
[13] A. Inoue, *Stabilization of metallic supercooled liquid and bulk amorphous alloys*, Acta Mater. 48 (2000), pp. 279–306.
[14] F.C. Frank and J.S. Kasper, *Complex alloy structures regarded as sphere packings. I. Definitions and basic principles*, Acta Cryst. 11 (1958), pp. 184–190.